

Heat Treatment Effect on Microstrain and Electrochemical Performance of Nano-sized FeS₂ Cathode for Thermal Batteries

Seung-Ho Kang^{1,2}, Jungmin Lee², Tae-Uk Hur², Hae-Won Cheong^{2,*}, and Junsin Yi^{1,*}

¹ College of Information and Communication Engineering, Sungkyunkwan University, Suwon 400746, Korea

² Agency for Defense Development, Daejeon 305600, Korea

*E-mail: imchw@add.re.kr, junsin@skku.edu

Received: 28 February 2016 / Accepted: 5 April 2016 / Published: 4 May 2016

Iron pyrite (FeS₂) is the most widely used material for cathodes in thermal batteries, attributed to its high specific energy density and natural abundance as well as low cost. In this study, nano-sized FeS₂ powders were synthesized by high-energy milling to improve electrochemical performance Li(Si)/FeS₂ thermal battery, and their particle sizes, microstrain, and thermal stabilities were investigated by particle size analysis (PSA), X-ray diffraction (XRD), and thermogravimetric analysis (TGA). Electrochemical performance was evaluated by single-cell discharge tests. The average particle size decreased from 107 μm to 261 nm after 10 h of dry milling, resulting in microstrain on FeS₂. This microstrain led to the thermal instability of the FeS₂ powder, causing an increase of the open-circuit voltage of Li(Si)/FeS₂ single cells. The voltage was stabilized from 2.45 V to 1.93 V, and thermal instability was mitigated by the heat treatment of the FeS₂ powder up to 400°C. The electrochemical performance of the single cells fabricated with nano-sized FeS₂ thermally annealed at 400°C improved by 57% as compared with that of untreated ones at a cut-off voltage of 1.4 V.

Keywords: Thermal battery, Iron pyrite, Microstrain, Heat treatment, Electrochemical performance

1. INTRODUCTION

Thermal batteries are primarily used as power sources for military applications, such as in missiles, torpedoes, and munitions, attributed to their excellent performance, robustness, and reliability [1, 3, 4]. A Li(Si)/FeS₂ couple is the most popular thermal battery system, and in 1978, Schneider and Bowser have reported a patent on the use of pyrite as the cathode in high-temperature batteries [2]. Masset and Guidotti have intensively examined the physicochemical properties and electrochemical performance of pyrite (FeS₂) material, such as discharge mechanisms and self-discharge phenomena [1,

3]. FeS₂ meets most of the requirements for cathode materials for use in thermal batteries, such as redox potential, high thermal stability, electrical conductivity, and low solubility in electrolyte [3].

Studies have been reported on the improvement of the energy density and power density of thermal batteries using CoS₂ [4] and NiS₂ [4, 5] as new cathode materials, as well as the methods of fabrication for new electrodes, such as thermal spray techniques [9, 10]. Simultaneously, studies have been reported on the use of fine FeS₂ particles for the improvement of electrochemical properties in primary batteries [6, 7, 8] and secondary batteries [11, 12]. Au has synthesized nanostructured FeS₂ powders and reported that the energy density of thermal batteries is two times that of micron-size powders, and the robustness of pellets is also significantly increased [13].

In this study, we fabricated nano-sized FeS₂ powders by high-energy milling under wet and dry conditions by varying milling time. Material properties of the powders were characterized by particle size analysis (PSA), X-ray diffraction analysis (XRD), and thermogravimetric analysis (TGA). In addition, we investigated the effect of heat treatment on the thermal stability of FeS₂ powders and evaluated the discharge performance of Li(Si)/FeS₂ single cells fabricated with thermally annealed nano-sized FeS₂.

2. EXPERIMENT DETAILS

2.1 Preparation of Nano-sized FeS₂ Powders

Nano-sized FeS₂ powders for cathodes were fabricated by high-energy ball milling (Planetary Micro Mill, FRITSCH) from its starting material (45–100 μm, 98% pure, LinYi) under wet and dry conditions. AA yttria-stabilized zirconia (YSZ) ball with a diameter of 3 mm was used for pulverizing the raw materials, and the ball-to-powder weight ratio (BPR) was 5:1. The milling speed was fixed at 600 rpm, and the milling time was varied from 1 h to 20 h.

2.2 Characterization

A PSA (HELOS/RODOS, Sympatec GmbH) system was employed for examining the particle size distributions of the FeS₂ powders after high-energy milling. Thermogravimetric analysis (TGA; Mettler-Toledo) was performed for verifying the thermal decomposition temperature of pulverized FeS₂ powders and finding the optimal temperature of heat treatment. The temperature was ramped up to a heating rate of 10°C min⁻¹ up to 700°C, and the weight of the sample was 10 mg. XRD (D8-Advance) was employed for investigating the phase identification and structural changes of pulverized FeS₂ powders using Cu K_α radiation, and the XRD patterns used for structural refinements were collected in the 2θ range of 10°–130° at a step size of 0.01° and a step time of 1 s. The peak position 2θ, full-width at half-maximum (FWHM), was obtained from the XRD spectra, and microstrain was analyzed by TOPAZ software using the Lorentzian function.

2.3 Preparation of Electrode Materials and Pellets

Cathode powders consisted of 73.5 wt% nano-sized FeS₂ (D₅₀ = 261 nm), 25 wt% eutectic salt mixture (LiCl 29.24 wt%–KCl 35.76 wt%/MgO 35 wt%), and 1.5 wt% Li₂O (<250 μm, 97% pure, Sigma-Aldrich). Li₂O was added as the lithiation agent for avoiding voltage spikes, which frequently occur with FeS₂, at the early transient discharge state [1, 4]. The homogeneous coating of the eutectic salt on FeS₂ particles by heat treatment enhances binding characteristics between pyrite particles. Lithium oxide also enhances the wettability of the molten salt and strengthens the compacted pellets [14]. MgO (<300 nm, 99% pure, Scora) powder was added as the retention agent for holding the molten electrolyte. The homogeneously mixed cathode powder with molten salt was fused at 400°C for 2 h under argon, followed by grinding and sieving.

The anode material comprised 75 wt% of Li(Si) alloys (Li 44.53 wt%–Si 55.47 wt%, Beijing General Research Institute), with 25 wt% of the eutectic salt LiCl–KCl (LiCl 45 wt%–KCl 55 wt%). The ternary eutectic salt LiCl–LiBr–LiF (LiCl 22 wt%–LiBr 68.4 wt%–LiF 9.6 wt%) was selected as the electrolyte for high-current-density applications.

Pellets with a diameter of 30 mm for electrodes and the solid electrolyte were prepared by conventional cold pressing. Anode (0.34 g, Li(Si)/LiCl–KCl) and electrolyte (0.70 g/LiCl–LiBr–LiF) powders were pressed into a pellet under static compaction pressures of 2.94 ton cm⁻² and 2.47 ton cm⁻², respectively. The measured thickness and geometrically calculated density of the anode pellets were 0.48 mm and 1.04 g cm⁻³ and those of the electrolyte pellets were 0.44 mm and 2.31 g cm⁻³, respectively. Cathode powders (0.72 g, FeS₂/LiCl–KCl/Li₂O) were also fabricated by conventional cold pressing into a pellet under a static compaction pressure of 5.89 ton cm⁻². The measured thickness and calculated density were 0.33 mm and 3.21 g cm⁻³, respectively. Table 1 lists the properties of the electrode pellets. For preventing the oxidation and contamination of each electrode material, all powder processing, pellet fabrication, and single-cell assemblies were prepared under dry air conditions of a relative humidity of less than 2%.

Table 1. Properties of electrode pellets.

Electrodes	Cathode	Electrolyte	Anode
Weight (g)	0.72	0.70	0.34
Outer diameter (mm)	30.60	30.61	30.60
Density (g cm ⁻³)	3.21	2.31	1.04
Compaction pressure (ton cm ⁻²)	5.89	2.47	2.94

2.4 Evaluation of Discharge Performance

Li(Si)/FeS₂ couples, with Li(Si) and FeS₂ as the anode and cathode, respectively, were adopted in this system for their high stability as well as current capability. Cathodes with nano-sized FeS₂ particles were fabricated with the same weight, diameter, and static pressure. The cathode, electrolyte, and anode pellets were stacked for single-cell assemblies, and the assemblies were inserted into a

specially designed temperature-controlled heating press. For evaluating discharge performance, consecutive pulse currents with current densities of 810 mA cm^{-2} (0.5 s) and $1,110 \text{ mA cm}^{-2}$ (0.5 s) were applied. Voltage data were directly measured using current collectors, and current data were measured using a shunt resistor (221501, Yokogawa). All test data were collected at a sampling frequency of 100 Hz using a data acquisition system (DaqBook2005, IOtech).

3. RESULTS AND DISCUSSION

3.1 Pulverization of FeS_2 Powder

Nano-sized FeS_2 powder was fabricated by high-energy milling by changing the milling time from 1 h to 20 h at a constant milling speed of 600 rpm. Fig. 1 shows the average particle sizes, $\langle D_{50} \rangle$, of FeS_2 powders synthesized by high-energy milling as a function of milling time under wet conditions. $\langle D_{50} \rangle$ rapidly decreased during the first hour of milling, down to around $1.02 \mu\text{m}$ (Fig. 1). With further milling, $\langle D_{50} \rangle$ slowly decreased, to values slightly below 542 nm after 20 h of milling. For obtaining finer particles, FeS_2 powders were pulverized under dry conditions; however, fine FeS_2 particles underwent agglomeration. For preventing this agglomeration of fine FeS_2 particles and for improving the electrical conductivity of the cathode pellet, 4 wt% of graphite (CB) was added as a lubricant. After the addition of graphite, no agglomeration was observed. The FeS_2 particles were homogeneously mixed with graphite, and $\langle D_{50} \rangle$ decreased to 261 nm in 10 h (Fig. 2). High-energy milling under dry conditions, as compared with wet conditions, with the addition of 4 wt% CB was significantly more effective for decreasing the particle size and milling time, attributed to its high potential energy and zero fluid friction force.

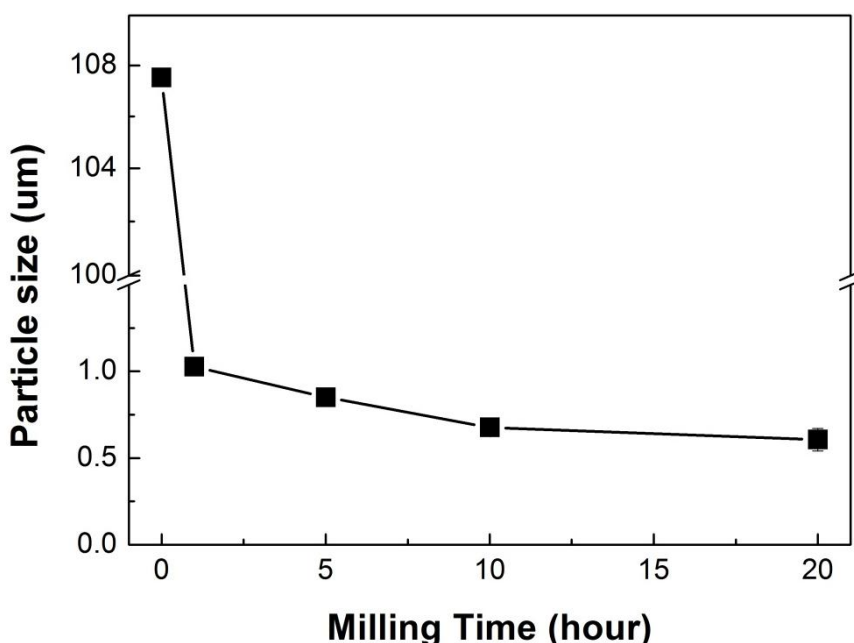


Figure 1. Average particle sizes of FeS_2 powders (wet condition)

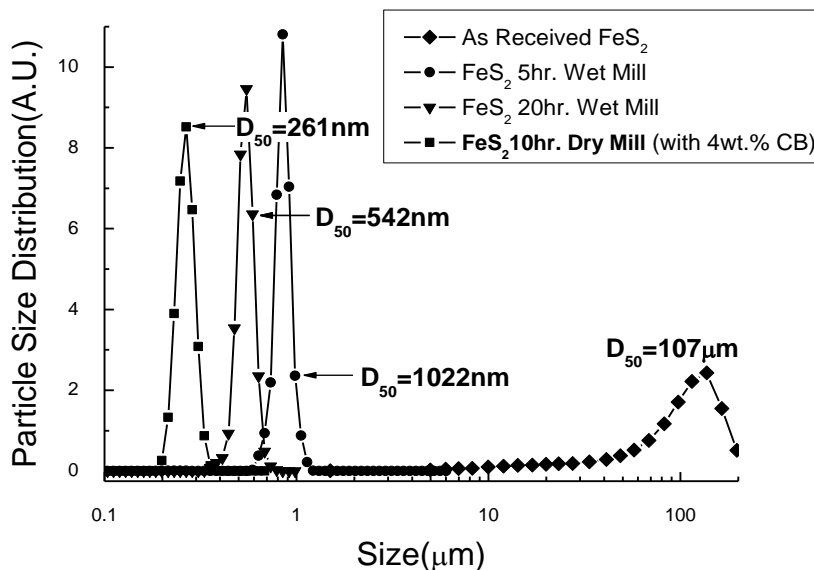


Figure 2. Comparison of particle size distributions (wet and dry conditions)

3.2 Effect of Heat Treatment on Microstructural Relaxation

Fig. 3 shows the XRD patterns of the FeS₂ powders synthesized by high-energy milling; only Bragg reflections of FeS₂ were observed, suggesting that the starting material does not undergo a significant reaction during and after milling (Fig. 3). From the XRD pattern, the initially sharp diffraction lines were broadened after high-energy milling, attributed to the milling energy pumped into the FeS₂ powders; this in turn resulted in the decrease of the particle size and an increase of internal lattice strains [15]. In other words, a part of the milling energy was utilized for pulverizing the FeS₂ particles, while another part was utilized for creating the defects such as lattice distortion [16].

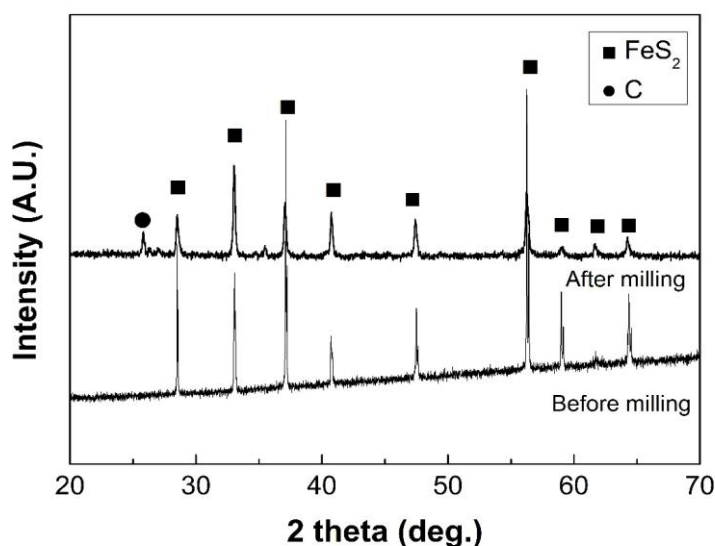


Figure 3. XRD patterns of FeS₂ powders after high-energy milling

Figs. 4 and 5 show the XRD patterns and the variation of microstrain on FeS₂ powders synthesized after 10 h of milling based on heat treatment temperature. With increasing temperature up to 400°C, the phase of fine FeS₂ particles did not change, and the broadening of diffraction lines slightly decreased. On the other hand, the FeS phase was observed by heat treatment at 500°C (Fig. 4), indicating that FeS₂ decomposes into non-stoichiometric monosulfide (pyrrhotite) and sulfur gas, as shown in Eq. (1) [17, 18]:



The microstrain induced by the milling energy decreased with increasing temperature of heat treatment up to 400°C from 0.091% to 0.062%, attributed to heat treatment (Fig. 5). This result is indicative of the mitigation of the thermal instability of nano-sized FeS₂ powder. From the XRD patterns and microstrain analysis, we conclude that the microstrain induced by milling energy decreases by heat treatment, which is in good agreement with the results reported previously [19, 20].

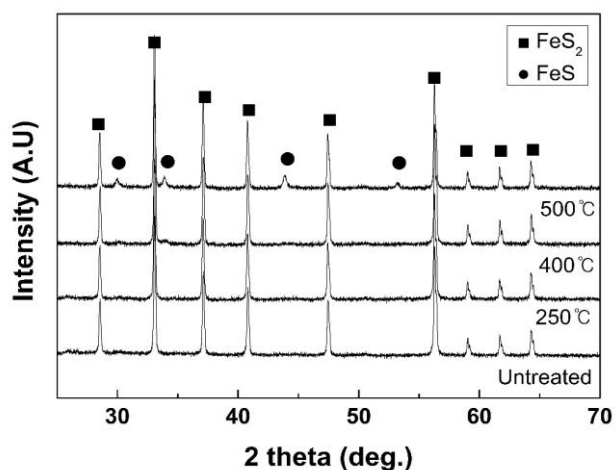


Figure 4. XRD patterns of FeS₂ powders after heat treatment

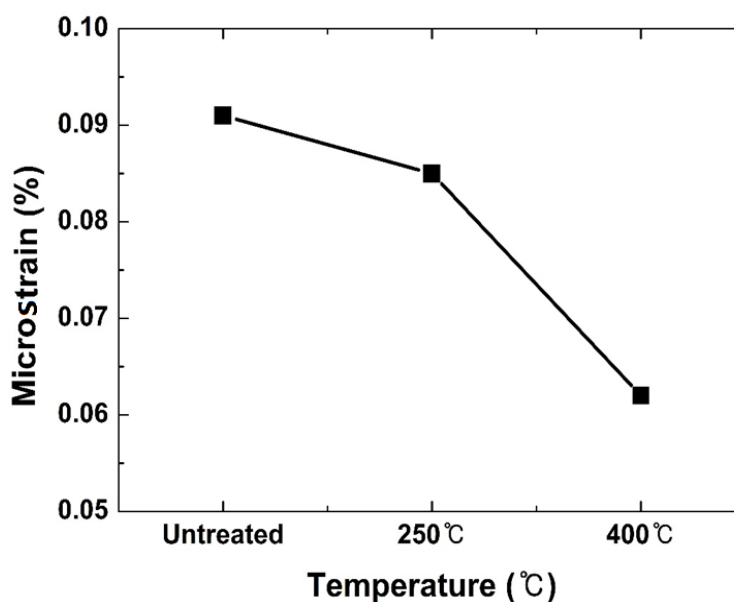


Figure 5. Microstrain of heat-treated FeS₂ powders

3.3 Thermal Stabilities of Nano-sized FeS₂ Powder

The thermal decomposition of FeS₂ starts at temperatures greater than 550°C under inert gas, resulting in the formation of a non-stoichiometric monosulfide (pyrrhotite) and sulfur vapor [17, 19]. Any released sulfur vapor from FeS₂ can react very exothermically with the Li-alloy anodes in the battery, which decreases the battery capacity, generates more heat, and accelerates the thermal decomposition of FeS₂, resulting in the destruction of the battery if thermal runaway occurs [1, 3].

Fig. 6 shows the TGA traces of FeS₂ powders after high-energy milling based on heat treatment temperature under argon. As compared with the decomposition temperature of FeS₂ previously reported [3, 17], the progressive decomposition of the powders produced by high-energy milling was observed from a low temperature. From the TGA traces, the stability of the powder heat-treated at 400°C was greater than those of both powders heat-treated at 250°C and untreated ones up to 500°C, which corresponds to the operating temperature of thermal batteries. Furthermore, the powders heat-treated at 250°C and untreated powders exhibited similar traces. The weight losses of the powders heat-treated at 400°C and 250°C were 11.7% and 13.9% at 500°C, respectively. After heat-treatment of up to 700°C, FeS₂ powders were completely decomposed into FeS and sulfur gas, and the weight losses of the untreated powder and those heat-treated at 250°C, 400°C, and 700°C were 27.8%, 29.2%, and 27.8%, respectively. This result is in accordance with electrochemical stoichiometry. On the other hand, the weight loss of the FeS₂ powder heat-treated at 500°C was 21.2% at 700°C, attributed to the thermal decomposition of FeS₂ during heat treatment; this thermal decomposition was evidenced by FeS peaks observed in the XRD patterns (Fig. 4).

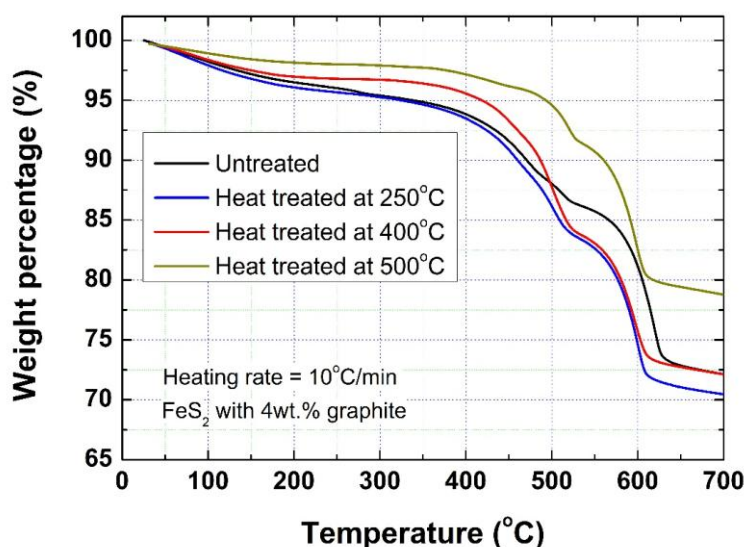


Figure 6. TGA curves of FeS₂ powders

From the XRD patterns (Fig. 5) and TGA traces (Fig. 6), the thermal stabilities of FeS₂ powders synthesized by high-energy milling increased with heat treatment temperatures of up to 400°C, and the optimal heat treatment temperature of the nano-sized FeS₂ powder synthesized by high-energy

milling was 400°C. This heat treatment is strongly recommended before the fabrication of pellets for the purpose of increasing the thermal stability of nano-sized FeS₂ powders.

3.4. Evaluation of Discharge Performance

For evaluating the discharge performances of single cells fabricated with the nano-sized FeS₂ powder, electrochemical discharging was conducted under consecutive pulse currents at 500°C. Fig. 7 shows the discharge performances of Li(Si)/FeS₂ single cells. The open-circuit voltage (OCV) of a single cell fabricated with untreated FeS₂ powders was relatively high (2.45 V), and with the increase in the heat treatment temperature up to 400°C, the OCV stabilized to 1.93 V. The superfluous high OCV of single cells caused by the thermal instability of nano-sized FeS₂ cathode can be understood by the microstrain induced by the milling energy. This result is in good agreement with the relaxation of the microstrain on nano-sized FeS₂ powders by heat treatment (Fig. 5).

At a cut-off voltage of 1.4 V, the capacities of single cells fabricated with cathode powders untreated and those heat-treated at 250°C were 0.74 equiv. Li per mol and 0.86 equiv. Li per mol, respectively, attributed to thermal instability, and the boundary between the 1st and 2nd plateaus was not clear. On the other hand, for the single cell fabricated with FeS₂ powder heat-treated at 400°C, the capacity was extended up to 1.15 equiv. Li per mol, attributed to the increased thermal stability. The 1st and 2nd plateaus were clearly observed during discharging, which might be used for extending cell capacity. These results are in good agreement with those obtained from thermogravimetric analysis (Fig. 6).

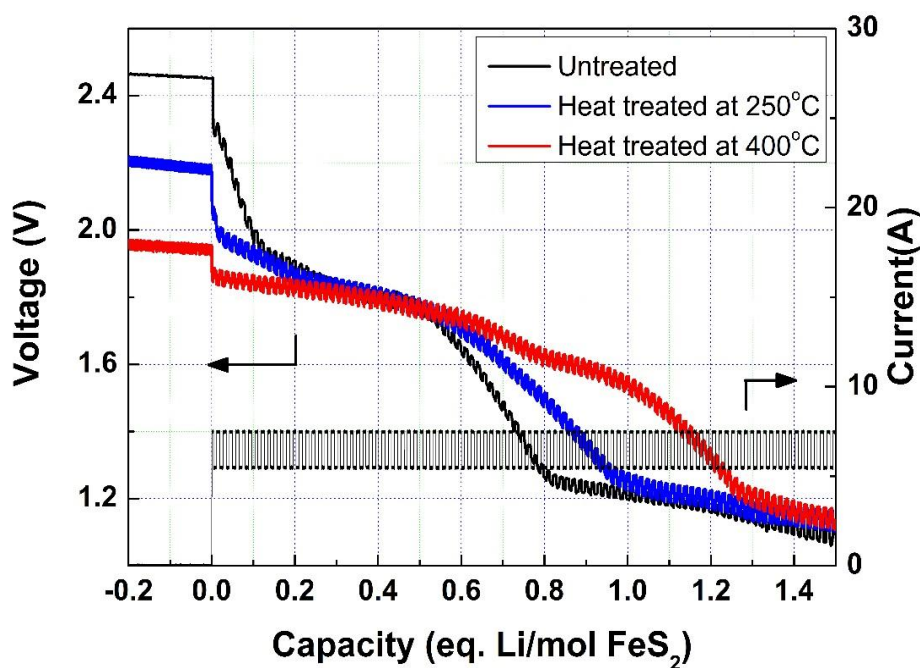


Figure 7. Discharge performances of Li(Si)/FeS₂ single cells

4. CONCLUSIONS

In this study, FeS₂ powders were synthesized by high-energy milling under both dry and wet conditions. The results obtained show that high-energy milling under dry conditions, as compared with wet conditions, and with the addition of 4 wt% of graphite was effective for decreasing average particle size and milling time. Microstrain induced by milling was mitigated with increasing heat treatment temperature up to 400°C, resulting in the stabilization of the open-circuit voltage from 2.45 V to 1.93 V and the increase of the thermal stability of single cells. At a cut-off voltage of 1.4 V, the discharge performance of single cells fabricated with the heat-treated nano-sized FeS₂ powders was remarkably improved as compared with that of single cells fabricated with untreated FeS₂ powders.

References

1. R. A. Guidotti and P. Masset, *J. Power Sources*, 161 (2006) 1443
2. A. A. Schneider and G. C. Bowser, *Thermal Battery Having Iron Pyrite Depolarizer*, U.S. Patent 4,119,769, October 10 (1978).
3. P. J. Masset and R. A. Guidotti, *J. Power Sources*, 177 (2008) 595
4. P. J. Masset and R. A. Guidotti, *J. Power Sources*, 178 (2008) 456
5. Z. Yang, X. Liu and Y. cui, *ECS Trans.*, 61 (2014), 9
6. Y. Shao-Horn, S. Osmialowski and Q. C. Horn, *J. Electrochem. Soc.*, 149 (2002) A1499
7. Y. Shao-Horn and Q. C. Horn, *Electrochem. Acta*, 46 (2001) 2613
8. H. Zhao, S. Wang, L. Fan and J. Wu, *Funct. Matter. Lett.*, 07 (2014) 1350069
9. D. E. Reisner, H. Ye, T. D. Xiao, R. A. Guidotti and F.W. Reinhardt, *J. New Mat. Electrochem. Syst.*, 2 (1999) 279
10. R. A. Guidotti, F. W. Reinhardt, J. Dai, J. Roth, and D. E. Reisner, *J. New Mat. Electrochem. Syst.*, 5 (2002) 273
11. D. Zhang, Y. Mai, J. Xiang, X. Xia, Y. Qiao and J. Tu, *J. Power Sources*, 217 (2012) 229
12. T. S. Yoder, M. Tussing, J. E. Cloud, Y. Yang, *J. Power Sources*, 274 (2015) 685
13. M. Au, *J. Power Sources*, 115 (2003) 360
14. H. Cheong, S. Kang, J. Kim and S. Cho, *J. Ceram. Process. Res.*, 13 (2012) s198
15. P. Pourghaharamani and E. Forssberg, *Int. J. Miner Process.*, 79 (2006) 106
16. T. P. Yadav, R. M. Yadav and D.P. Singh, *Nanosci. Nanotechnol.*, 2 (2012) 22
17. P. J. Masset, *ECS Trans.*, 25 (2010), 155
18. P. J. Masset, *Z. Naturforsch.*, 63a (2008) 596
19. G. R. Khayati and K. Janghorban, *Trans. Nonferrous. Met. Soc. China*, 23 (2013) 543
20. D. M. Blanco, P. Gorria, J. A. Blanco, M. J. Perez and J. Campo, *J. Phys. Condens. Matter*, 20 (2008) 335213